The ribosome-associated complex regulates cytosolic translation upon mitoprotein-induced stress

Jiaxin Qian [1], Annika Nutz [2], Katja Hansen [2], Lea Bertgen [2], Mirita Franz-Wachtel [3], Boris Macek [3], Johannes M. Hermann [2], and Doron Rapaport [1,*]

[1] Interfaculty Institute of Biochemistry, University of Tübingen, 72076 Tübingen, Germany

[2] Cell Biology, University of Kaiserslautern, Kaiserslautern, Germany.

[3] Proteome Center Tübingen, University of Tübingen, 72076 Tübingen, Germany

* To whom correspondence should be addressed:

Interfaculty Institute of Biochemistry, University of Tübingen, Auf der Morgenstelle 34, 72076 Tübingen, Germany. Tel: +49-7071-2974184; E-mail: doron.rapaport@uni-tuebingen.de. ORCID: 0000-0003-3136-1207

Runing title: RAC regulates mitoprotein-induced stress

Abstract

The biogenesis of mitochondria relies on the import of newly synthesized precursor proteins from the cytosol. Tom70 is a mitochondrial surface receptor which recognizes precursors and serves as an interface between mitochondrial protein import and the cytosolic proteostasis network. Mitochondrial import defects trigger a complex stress response, in which compromised protein synthesis rates are a characteristic element. The molecular interplay that connects mitochondrial (dys)function to cytosolic translation rates in yeast cells is however poorly understood. Here, we show that the deletion of the two Tom70 paralogs of yeast (*TOM70* and *TOM71*) leads to defects in mitochondrial biogenesis and slow cell growth. Surprisingly, upon heat stress, the deletion of *ZUO1*, a chaperone of the ribosome-associated complex (RAC), largely prevented the slow growth and the reduced translation rates in the *tom70Δ/tom71Δ* double deletion mutant. In contrast, the mitochondrial defects were not cured but even enhanced by *ZUO1* deletion. Our study shows that Zuo1 is a critical component in the signaling pathway that mutes protein synthesis upon mitochondrial dysfunction. We propose a novel paradigm according to which RAC serves as a stress-controlled regulatory element of the cytosolic translation machinery.

Key words: mitochondria, protein import, proteostasis, ribosome-associated complex, Tom70

Introduction

Mitochondrial proteins are mostly synthesized in the cytosol and then must be imported into the organelle via a set of complex processes involving multiple factors and pathways [1]. Cytosolic chaperones and their co-chaperones, particularly those from the Hsp40, Hsp70 and Hsp90 families, contribute to these pathways by maintaining mitochondrial precursor proteins in an import-competent conformation [2-5]. These (co)chaperones not only prevent aggregation and misfolding of newly synthesized proteins in the cytosol, but also ensure they are properly delivered to and inserted into the mitochondria [6]. Such interactions with (co)chaperones keep the precursor proteins in a loosely folded, unfolded, or partially folded conformation that is compatible with the import machinery [7]. The initial interactions with surface import receptors are essential for the specific recognition of the mitochondrial precursor proteins and for their subsequently efficient translocation across the mitochondrial membranes.

We and others observed that the mitochondrial surface receptors Tom70 and its paralogue Tom71 contribute to the recognition of newly synthesized mitochondrial proteins and in addition serve as a docking site for cytosolic (co)chaperones on the surface of the organelle [2-4] [8, 9]. Furthermore, Tom70 was recently reported to be involved in the localized condensation of protein aggregates on the mitochondrial surface [10]. Both Tom70 and Tom71 are anchored to the mitochondrial outer membrane via a single transmembrane segment at their N-terminal region and contain multiple tetratricopeptide repeat (TPR) domains [11, 12]. Tom70 plays a crucial role particularly in recognizing and importing precursor proteins with internal targeting sequences like multispan membrane proteins residing in both mitochondrial membranes and matrix destined proteins with internal mitochondrial targeting signal (iMTS) [13-15]. Tom71, a less abundant paralogue of Tom70, shares sequence similarity with Tom70, but its precise molecular function is still being investigated [16-18].

In line with their central role in import of mitochondrial proteins, the combined absence of both Tom70 and Tom71 causes proteostasis stress in the cytosol [2]. Such a stress manifests as accumulation of misfolded or unfolded mitochondrial precursor proteins in the cytosol, triggering cytosolic responses and potentially leading to cell damage if not resolved [19, 20]. To reduce such cytosolic proteostasis stress, cells developed a combined approach targeting protein synthesis, folding, and degradation [21-24]. Such an adaptation involves optimizing the ubiquitin-proteasome system (UPS), promoting proper protein folding, and regulating protein synthesis. The latter element is currently understudied, and it is unclear how

77 changes in cytosolic proteostasis and mitoprotein induced stress in yeast cells can influence the
78 quantity and quality of protein synthesis.

79 A potential player in translation regulation is Zuo1, also known as Zuotin, a ribosome-
80 associated J-protein with multiple functions [25, 26]. It primarily acts as a co-chaperone for
81 Hsp70 (Ssb1) forming together with another Hsp70 (Ssz1) the ribosome-associated complex
82 (RAC) [27], assisting in the co-translational folding of nascent polypeptides [28]. Additionally,
83 Zuo1 plays a role in ribosome biogenesis, DNA repair, rRNA processing, and the regulation of
84 translation [29-31].

85 In the current study we investigated the interplay between the mitochondrial surface receptors
86 Tom70/71 and the co-chaperone Zuo1. Surprisingly, we observed that, at elevated
87 temperatures, the absence of Zuo1 improves the growth of cells deleted for Tom70/71 and
88 accelerates translation in this double deletion strain. The absence of Zuo1 resulted also in a
89 reduction in the levels of cytosolic stress chaperones like Hsp42 and Hsp26. Thus, we
90 discovered a Zuo1-mediated crosstalk between accumulation of mitochondrial precursor
91 proteins and regulation of cytosolic translation.

92

93

94 ## Results

95 ### The deletion of *ZUO1* has temperature-dependent effect on growth of yeast cells

96 To better understand the crosstalk between Zuo1 and the proteostasis of mitochondrial
97 precursor proteins, we aimed to test the effect of the deletion of *ZUO1* on the growth of yeast
98 cells under various conditions. To achieve that aim, we monitored growth on different carbon
99 sources, at various temperatures, and in combination with mitoprotein-induced stress. We
100 observed that the deletion of *ZUO1* resulted in a slower growth on fermentable carbon sources
101 like glucose or galactose as well as on the non-fermentable carbon source glycerol (Fig. 1A-
102 C). These results are in line with previous studies reporting a growth retardation of *zuo1Δ* cells
103 at 30°C on glucose-containing media [25, 26]. To create cytosolic accumulation of non-
104 imported mitochondrial proteins, we deleted the import receptor Tom70 and its less studied
105 paralogue, Tom71. This double-deletion resulted in minorly retarded growth at 30°C on the
106 tested carbon sources (Fig. 1A-C). Importantly, a triple deletion strain (*tom70Δ/tom71Δ/zuo1Δ)*
107 showed a genetic negative interaction and grew much slower than the tested single or double

108 deletion strains (Fig. 1A-C). These findings suggest that under normal temperature a functional
109 Zuo1 is beneficial when the mitochondrial proteins Tom70/71 are absent.

110 Next, we asked whether increasing stress by growing the cells at an elevated temperature
111 (37°C) will change the behavior of the mutated strains. As expected [2], cells lacking both
112 import receptors hardly grew under these conditions, while the single deletion of *ZUO1* had
113 only a mild growth defect (Fig. 2A-C). Surprisingly, the deletion of the J-protein in the strain
114 lacking both receptors (*tom70Δ/tom71Δ)* resulted in cells that grew much better than the
115 original double deletion strain (Fig. 2A-C). Importantly, this improvement in growth was
116 observed on solid medium containing glucose, galactose, or glycerol as well as in liquid
117 medium harboring either glucose or galactose. The growth enhancement upon deletion of
118 *ZUO1* was detected also in combination with the single deletion of *TOM70* (Fig. 2A-C). In
119 summary, at elevated temperature the absence of Zuo1 promotes the viability of cells that suffer
120 from mitoprotein-induced stress.

121 **Cells lacking Zuo1 have altered proteome**

122 To understand the cellular events that resulted in this unexpected benefit of cells deleted for
123 *ZUO1*, we compared by an unbiased approach the proteome of the mutated cells to those of
124 control cells. To this goal, we isolated proteins from control (WT), double deletion
125 (*tom70Δ/tom71Δ),* and triple deletion cells (*tom70Δ/tom71Δ/zuo1Δ)* grown at 37°C on glucose
126 containing medium and analyzed them by mass spectrometry (Fig. 3A). This analysis indicated
127 a unique protein composition of the different cell types and a similar coverage of the yeast
128 proteome among the investigated cells (Fig. 3B-C). Initially, we compared the proteome of the
129 control cells to that of the double deletion ones. As observed before for *tom70Δ/tom71Δ* cells
130 [2], they harbor reduced amounts of many mitochondrial proteins, among the most affected
131 ones are Coq2 and Mdm36 (Fig. 3D-F and Suppl. Table 1). Similarly, also the triple deletion
132 cells contained, as compared to control cells, less mitochondrial proteins where the levels of
133 subunits of the respiratory chain complexes and mitochondrial ribosomes as well as
134 mitochondrial inner membrane proteins were specially reduced (Fig. 3F and Suppl. Table 1).

135 A specific group of yeast genes are expressed under the control of a dedicated heat response
136 program (Fig. 4A and Suppl. Table 2) [32]. The protein products of these genes are often
137 involved in counteracting cytosolic proteins aggregation and misfolding. Thus, we were
138 particularly interested in the expression of such proteins in the different examined strains. In
139 agreement with the enhanced protein aggregation upon absence of Tom70/71, we detected

140 elevated levels of the small chaperones Hsp12 and Hsp26 in these cells (Fig. 4B-D). Of note,
141 comparison of the triple deletion strain with the control cells revealed that these increased
142 expression levels were mainly diminished for Hsp26 and the levels of Hsp12 were even lower
143 than the control cells (Fig. 4B-D). This trend was not observed for all cytosolic chaperones and
144 the amounts of the rather generic chaperone Hsp82 were higher in the triple deletion strain as
145 compared to control or the double deletion cells (Suppl. Table 1). Hence, our findings hint to a
146 remodeling of the cytosolic stress response upon deletion of *ZUO1*.

147 Next, we aimed to confirm our mass spectrometry findings by an unrelated method. To this
148 end, we analyzed the protein extracts of the investigated cells, grown on glucose at 37°C, by
149 SDS-PAGE followed by immunostaining. Indeed, we could verify that the double deletion of
150 *TOM70/71* caused a significant increase in the amounts of cytosolic chaperones with anti-stress
151 activity like Hsp12, Hsp26, and Hsp104. Notably, these elevated levels were reduced back to
152 normal levels upon the additional deletion of *ZUO1* on top of the absence of Tom70/71 (Fig.
153 5A-B). Interestingly, the amounts of general chaperones like Hsp70 (Ssa1) or Hsp90 (Hsp82)
154 did not change much among the various strains. Similarly unchanged were the amounts of the
155 unrelated cytosolic proteins Bmh1 and hexokinase (Hxk) 1 (Fig. 5A-B).

156 Since most of the mitochondrial outer membrane (MOM) proteins were reported to be
157 substrates of Tom70/71, we also monitored their amounts in the various strains. While some
158 proteins (like Tom20, Tom40, Msp1 and Fis1) were only mildly affected or not at all, the levels
159 of others were dramatically altered. For example, the absence of Tom70 alone or in
160 combination with Tom71 resulted in a major reduction in the levels of the β-barrel protein Porin
161 (VDAC1). This reduction was partially compensated by the additional deletion of *Zuo1* (Fig.
162 6A-B). However, the absence of Zuo1 did not have the same effect on all proteins. A somewhat
163 different pattern was observed for another β-barrel protein, Tob55/Sam50 where the absence
164 of Zuo1 did not enhance the compromised levels upon the removal of Tom70 or Tom70/71
165 (Fig. 6A-B).

166 A completely distinctive picture emerged for three proteins (Om45, Om14, and Mcr1) that were
167 suggested to participate in mitochondrial metabolic processes. Against our expectations, the
168 double deletion of Tom70 and Tom71 resulted in enhanced amounts of these proteins.
169 However, the additional deletion of *ZUO1* caused a dramatic decrease in the amounts of these
170 proteins to a level much below that in control cells (Fig. 6A-B). Taking together, the western
171 analysis demonstrated individual effects for the absence of Zuo1 on the levels of various MOM
172 proteins.

173 **The absence of Zuo1 enhances translation and changes the pattern of cytosolic aggregates**

174 The aforementioned observations encouraged us to investigate the contribution of Zuo1 to
175 additional cellular processes like the formation of cytosolic aggregates or translation. To
176 monitor the number of aggregates per cell we used a previously established method namely,
177 the staining of such aggregates with a disaggregase Hsp104 fused to GFP [33]. Using this
178 approach, we noticed that the single absence of Zuo1 resulted in a slight increase in the number
179 of cells with several aggregates. The double deletion of Tom70/71 resulted in even more cells
180 with many aggregates but, the additional deletion of *ZUO1* from *tom70Δ/tom71Δ* cells reduced
181 the number of aggregates per cell without affecting much the overall number of cells with any
182 number of aggregates (Fig. 7A-B).

183 Considering this observation, we wished to determine the effect of Zuo1 on translation. To
184 achieve this aim, we employed radioactive *in vivo* labeling followed by extracting proteins
185 from the cells and analyzing the newly synthesized proteins by either SDS-PAGE or dot blot.
186 Proteins were detected in both cases by autoradiography. Both assays revealed that the absence
187 of Zuo1 increases overall translation at 30°C and the dot blot assay expanded this finding also
188 to cells grown at 37°C (Fig. 7C-E). Collectively, these results indicate that the removal of Zuo1
189 from cells lacking Tom70/71 improves the growth of the latter cells probably by reducing the
190 number of aggregates per cell in combination with enhancing global protein synthesis.

191

192

193 ## Discussion

194 Defects in import of mitochondrial proteins have a well-documented impact on proteostasis in
195 the cytosol and are associated with protein aggregation diseases [23, 24, 34]. Thus,
196 understanding the mechanisms that contribute to proteostasis during inhibition in
197 mitochondrial protein import can shed new light on cellular stress responses. It is well
198 established that the absence of the mitochondrial surface proteins Tom70 and its paralogue
199 Tom71 causes defects in mitochondrial biogenesis combined with mitoprotein stress in the
200 cytosol [2]. This complex outcome is related to the double function of these proteins; they play
201 a role in recognition of newly synthesized mitochondrial proteins and serve as a docking site
202 for cytosolic (co)chaperones loaded with mitochondrial precursor proteins [3, 4, 35-37]. To
203 better understand the cellular importance of these proteins in the context of cellular stress, we

204 combined their absence with alteration of protein translation via deletion of the RAC subunit,
205 Zuotin (Zuo1).

206 Surprisingly, at elevated temperature, these triple deleted cells (*tom70Δ/tom71Δ/zuo1Δ)* grew
207 better than cells lacking only the two receptor proteins. This improved growth was
208 accompanied by less aggregates per cell and enhanced translation. The latter effect is especially
209 of interest because it is well known that the cytosolic stress response involves a coordinated
210 effort to reduce overall protein synthesis while simultaneously promoting the synthesis of
211 proteins essential for cell survival under stress conditions. This phenomenon, which is part of
212 the integrated stress response (ISR), helps cells to conserve energy and resources during stress
213 [38]. Indeed, we observed such differential alterations upon the deletion of *ZUO1*. Despite the
214 general trend of enhanced translation, we observed that the levels of the small chaperones
215 Hsp12 and Hsp26, which increased dramatically upon the deletion of *TOM70/71,* went down
216 upon the removal of Zuo1.

217 In human cells, the link between cytosolic proteostasis stress and regulation of proteins
218 synthesis often involves the translation initiation factor 2 subunit-α (eIF2α). It is well
219 established that an increased level of phosphorylation of eIF2α is a hallmark of the ISR. Stress-
220 activated kinases phosphorylate eIF2α, leading to a global reduction in protein synthesis
221 initiation [38, 39]. Mitochondrial stress is relayed to this system in mammalian cells via the
222 protein DELE1 (Deleted in Liver Cancer 1) [40]. When mitochondria experience stress,
223 DELE1, which is normally imported into the mitochondrial matrix, is cleaved by the OMA1
224 protease and translocates to the cytoplasm, where it interacts with HRI (Heme-regulated
225 inhibitor) kinase that subsequently phosphorylates eIF2α [40] [41]. However, despite this
226 wealth of knowledge about the mammalian system, it was unclear how mitochondrial-induced
227 stress is causing translation slowdown in yeast cells. Our findings shed light on this issue by
228 suggesting that Zuo1 is part of this missing link. It seems that under stress conditions Zuo1
229 contributes to the reduction of translation efficiency and therefore its absence under such
230 circumstances results in elevated protein synthesis rate (Fig. 7F).

231 Previous studies are not conclusive regarding the effect of Zuo1 on protein translation rate. One
232 work reported that the deletion of Zuo1 by itself or in combination with Arsen-induced stress
233 causes a reduction in global translation [42]. On the other hand, another report indicated that
234 while *zuo1Δ* cells have lower polysome levels in basal conditions [43], this does not seem to
235 affect the *in vivo* global translation rate [29]. Hence, it appears that Zuo1 might be involved in

236 fine-tuning translation in response to different signaling inputs and in accordance with the
237 proteostasis situation at the cytosol.

238 We observed that the absence of Tom70/71 causes increased number of cells with large number
239 of aggregates and elevated levels of the small stress proteins Hsp12 and Hsp26 [44, 45],
240 supporting their role as docking sites for substrate-associated chaperones [2]. However, the
241 absence of Zuo1 resulted, despite the enhanced global translation, in a reduced number of cells
242 with many aggregates and highly reduced levels of Hsp12 and Hsp26. These observations
243 further support the notion that Zuo1 can differentially affect the synthesis of various proteins.

244 Our proteomic approach clearly demonstrated that the deletion of Tom70/71 resulted, as
245 reported before, in compromised levels of many mitochondrial proteins. However, although
246 the further deletion of *ZUO1* on this background did not restore the levels of the mitochondrial
247 proteins, it did improve considerably the growth ability of the cells. These important findings
248 demonstrate that the main problem in cells lacking Tom70/71 is likely not the compromised
249 mitochondrial biogenesis but rather the cytosolic proteostasis stress. Deciphering the
250 mechanism by which the absence of Zuo1 counteracts this latter problem is an important
251 question that awaits future studies.

252

253

254

255

256

257

258 # Methods

259 ## Growth Curves

260 Yeast cells were precultured in glucose medium until the exponential phase was reached. Cells
261 equivalent to an OD_{600} of 1.0 were harvested for 1 min at 16000xg and resuspended in water.
262 Cells were diluted to an OD_{600} of 0.1 into media containing either glucose or galactose as a
263 carbon source. Cells were rotating at either 30°C or 37°C in a SPECTROstar^{Nano} plate reader
264 (BMG LABTECH) with the settings shaking between reads at 500 rpm and double orbital for
265 20-40 hrs. Three technical replicates were used per strain and condition. The data was
266 visualized in R.

267 **Monitoring Yeast Growth on solid medium**

268 Yeast cells were initially cultured overnight in 5 mL of glucose-containing medium. The
269 cultures were then diluted to an OD_{600} of 0.2–0.3 and incubated for further 2–4 hours until
270 reaching an OD_{600} of 0.8–1.5. Next, cells equivalent to 2.0 units of OD_{600} were collected and
271 resuspended in 1 mL of sterile water. A series of 1:10 serial dilutions were prepared, and 4 µL
272 of each dilution were spotted onto agar plates with the indicated carbon source. The plates were
273 incubated at different temperatures for further analysis.

274 **Whole cell lysates**

275 Cells were cultured at either 30°C or 37°C until they reached exponential phase (OD_{600} of 0.5-
276 1.5) and then 2-10 OD_{600} units were harvested for lysis. Cells were lysed by one of the
277 following options: (i) Cells were washed twice with water and resuspended in 30 µl loading
278 dye supplemented with 50 mM DTT. Cells were lysed for 5 min at 4°C with help of 4-5 glass
279 beads (diameter of 1 mm). Afterwards, samples were boiled for 5 min at 96°C and additional
280 50 µl loading dye with DTT was added. (ii) Alternatively, cells pellet was resuspended in 800
281 µL of 0.1 M NaOH and incubated for 5 min at room temperature (RT). After centrifugation
282 (13000 ×g, 1 min, RT), cells were resuspended in 50 µL of 2×loading dye containing 5% β-
283 mercaptoethanol. The samples were then incubated at 95°C for 3 min, centrifuged again
284 (13,000×g, 1 min, RT), and the supernatant was collected for further analysis. In both cases,
285 samples were analyzed by SDS-PAGE and immunostaining. Signals were detected using the
286 chemiluminescence mode and either the ChemiDoc MP Imaging System (BioRad) or
287 appropriate films.

288 **Trichloroacetic acid (TCA) precipitation of proteins**

289 Proteins were precipitated by adding 72% TCA to the solution to achieve a final concentration
290 of 12% TCA. The samples were incubated overnight at -20°C to ensure complete precipitation.
291 Proteins were sedimented by centrifugation (25,000xg, 30 min, 4°C) washed with ice-cold
292 acetone (-20°C) and pelleted again under the same conditions. The resulting protein pellets
293 were dried at RT and resuspended in sample buffer.

294 **Radioactive *in vivo* labeling of translation products**

295 Cells were cultured in glucose- or galactose-containing medium at 30°C or 37°C until reaching
296 the exponential growth phase and were then harvested for further analysis. For radioactive *in*
297 *vivo* labeling of translation products, cells of 1 OD_{600} unit were washed with synthetic glucose-
298 or galactose-containing medium lacking methionine. Radiolabeling was initiated by adding

299 ^{35}S-methionine (0.75 µl of an 11 µCi solution) to the suspension for incubation at the indicated
300 temperature for 2, 5, 10, or 15 min. The reactions were quenched by adding 8 mM cold
301 methionine in case of the dot blot experiment or cells were directly lysed after 5 or 15 min of
302 incubation. Cells were lysed using 0.3 M NaOH, 1% β-mercaptoethanol, and 2 mM
303 phenylmethylsulfonyl fluoride (PMSF), and proteins were precipitated with 12% TCA. The
304 samples were analyzed using SDS-PAGE or dot blotting.

305 For dot blot analysis, 5 µl of a 1:30 diluted sample was loaded onto a nitrocellulose membrane
306 using the SCR 96 Minifold I apparatus under vacuum. Radiolabeled proteins were detected by
307 autoradiography by exposing the dried membrane to an imaging plate (Fujifilm) and
308 visualizing it with Typhoon FLA 7000 phospho-imager (GE Healthcare) or on Super RX
309 Medical X-Ray Films (Fuji) using the Optimax Type developer (MS Laborgeräte). Images were
310 scanned in an 8-bit or 16-bit grayscale format, and signal intensities were quantified using
311 Image Lab software (BioRad). Normalization was performed based on the immunostaining
312 with antibodies against Rpl6B (antibody in a 1:2000 dilution) that served as a loading control,
313 and the wildtype (WT) sample labeled for15 minutes was set as 100%.

314 **Fluorescence microscopy**

315 Cells were transformed with a pYX142 Hsp104-GFP yeast expression plasmid [33]. Cells
316 equivalent to one unit of OD_{600} were harvested via centrifugation, and cell pellets were
317 resuspended in 30 µl of water. A small aliquot (3 µl) was pipetted onto a glass slide and covered
318 with a cover slip. Manual microscopy was performed using a Leica Dmi8 Thunder Imager,
319 with an external LED8 light source and a Leica DFC9000GTC camera. Images were acquired
320 using an HC PL APO 100x/1.44 Oil UV objective with Immersion Oil Type A 518 F, a
321 DFT51010 filter cube for GFP excitation at 475 nm at 540 MHz as quality mode at 16-bit and
322 saved in the Leica Image Format. The resolution was 2048x2048 pixels and a physical size of
323 132.03 µm. Image analysis was performed with LAS X software, and further processing was
324 conducted in Fiji/ImageJ. The number of Hsp104-GFP foci per cell was counted manually and
325 categorized into three groups: cells with no foci, 1–4 foci, or ≥5 foci per cell. The percentage
326 of cells in each category was calculated and the data were visualized using R.

327 **LC MS/MS**

328 Proteins were precipitated overnight at -20°C with an ice-cold acetone-methanol mixture. After
329 centrifugation (2000xg, 20 min, 4 °C), protein pellets were washed with 80% ice-cold acetone.
330 Pellet was dried, and proteins resolved in denaturation buffer (6 M urea, 2 M thiourea, 10 mM

331 Tris, pH 8.0). Protein concentration was determined with Bradford assay, and ten micrograms
332 of protein were subjected to in-solution digestion with trypsin as described previously [46].
333 Desalted peptides [47] were analyzed on a Vanquish Neo nano-UHPLC coupled to an Orbitrap
334 Exploris 480 mass spectrometer through a nano-electrospray ion source (all Thermo
335 Scientific): 0.25 µg peptides were loaded onto a 20 cm HPLC column with 75 µm inner
336 diameter (CoAnn Technologies, ICT36007508F-50) in-house packed with 1.9 µm ReproSil-
337 Pur C18-AQ silica beads (Dr. Maisch HPLC GmbH, r119.aq.) under pressure control (1000
338 bar). Elution was performed with a 45 min segmented gradient of 5-55% of HPLC solvent B
339 (80% acetonitrile in 0.1% formic acid) at a flow rate of 300 nl/min and a constant temperature
340 of 40°C. The mass spectrometer was operated in a positive ion and data-independent
341 acquisition (DIA) mode. MS1 spectra were acquired at a resolution of 120k in the range of m/z
342 400-1000 with automatic gain control (AGC) set to 300%, and maximum ion injection time
343 (MaxIT) set to auto. MS2 spectra were acquired in the range of m/z 145-1450 with a normalized
344 collision energy of 27% at a resolution of 30k, whereby AGC was set to 800%, and MaxIT was
345 set to auto. DIA isolation windows of 10 m/z (60 scan events) were defined as the window
346 placement optimization. The mass spectrometry proteomics data have been deposited to the
347 ProteomeXchange Consortium via the PRIDE partner repository with the dataset
348 identifier PXD067604.

349 **MS data processing**

350 DIA-based MS data were processed in directDIA+ mode using the Spectronaut software
351 version 19.5 (Biognosys) using default search parameters with more stringent identification
352 settings [48]. Spectra were predicted using a *Saccharomyces cerevisiae* database obtained from
353 Uniprot (downloaded 30th of January 2024; 6,091 entries). Results were exported using the
354 Pivot Report showing all identified and quantified protein groups.

355 These were further processed using the R programming language (R version 4.5.1,
356 https://www.R-project.org). For each condition, proteins that were identified in less than two
357 replicates were removed (N = 3). This resulted in 4254 total identified protein groups whose
358 quantities were log2-transformed, normalized using variance stable normalization [49], and
359 batch-cleaned using limma [50]. Lastly, missing values were imputed by sampling N = 3 values
360 from a normal distribution (seed = 127851) and using them whenever there were no valid
361 values in a triplicate of a condition. The mean of this normal distribution corresponds to the
362 1% percentile of label-free quantification (LFQ) intensities. Its standard deviation is
363 determined as the median of LFQ intensity sample standard deviations calculated within and

364 then averaged over each triplicate. Proteins were tested for differential expression using limma
365 for the indicated pairwise comparison of samples and a Benjamini-Hochberg procedure was
366 used to account for multiple testing. All relevant test results are listed in Suppl. Table 1.
367 Principal component analysis was carried out on the processed intensities by singular value
368 decomposition. For gene ontology (GO) enrichment analysis of depleted proteins, proteins with
369 smaller than −0.8 $\log_2$ fold change were used as target set and analyzed using the GOrilla tool
370 (http://cbl-gorilla.cs.technion.ac.il/) [51] with all quantified proteins as background set (Suppl.
371 Table 3).

372

373

374

375 **Conflict of interest**

376 The authors have no conflict of interest to report.

377

378 **Author Contributions**

379 J.Q., K.H. and L.B. planned and performed experiments and analyzed data; A.N. analyzed
380 data; M. F.-W. performed the mass spectrometry analysis; B.M. supervised analysis; J.M.H.
381 and D.R. planned experiments, analyzed data, and wrote the manuscript.

382

383 **Acknowledgments**

384 We thank E. Kracker for excellent technical assistance, K.S. Dimmer for helpful discussions,
385 and S. Rospert and J. Buchner for antibodies. This work was supported by the Deutsche
386 Forschungsgemeinschaft (RA 1028/11-1 to D.R. and HE 2803/11-1 to J.M.H), the European
387 Research Council (MitoCyto 101052639 to J.M.H.), and doctoral fellowship of the Chinese
388 Scholarship Council (CSC) to J.Q.

389

390

391

References

1. Endo, T. and N. Wiedemann, *Molecular machineries and pathways of mitochondrial protein transport.* Nat Rev Mol Cell Biol, 2025.
2. Backes, S., et al., *The chaperone-binding activity of the mitochondrial surface receptor Tom70 protects the cytosol against mitoprotein-induced stress.* Cell Rep, 2021. **35**(1): p. 108936.
3. Drwesh, L., et al., *A network of cytosolic (co)chaperones promotes the biogenesis of mitochondrial signal-anchored outer membrane proteins.* Elife, 2022. **11**.
4. Jores, T., et al., *Cytosolic Hsp70 and Hsp40 chaperones enable the biogenesis of mitochondrial beta-barrel proteins.* J Cell Biol, 2018. **217**(9): p. 3091-3108.
5. Hoseini, H., et al., *The cytosolic cochaperone Sti1 is relevant for mitochondrial biogenesis and morphology.* FEBS J, 2016. **283**(18): p. 3338-52.
6. Bykov, Y.S., et al., *Cytosolic Events in the Biogenesis of Mitochondrial Proteins.* Trends Biochem Sci, 2020. **45**(8): p. 650-667.
7. Rodl, S., et al., *A protein-specific priority code in presequences determines the efficiency of mitochondrial protein import.* PLoS Biol, 2025. **23**(7): p. e3003298.
8. Brix, J., et al., *The mitochondrial import receptor Tom70: identification of a 25 kDa core domain with a specific binding site for preproteins.* J Mol Biol, 2000. **303**(4): p. 479-88.
9. Papic, D., et al., *The role of Djp1 in import of the mitochondrial protein Mim1 demonstrates specificity between a cochaperone and its substrate protein.* Mol Cell Biol, 2013. **33**(20): p. 4083-94.
10. Liu, Q., et al., *Nascent mitochondrial proteins initiate the localized condensation of cytosolic protein aggregates on the mitochondrial surface.* Proc Natl Acad Sci U S A, 2023. **120**(31): p. e2300475120.
11. Li, J., et al., *Molecular chaperone Hsp70/Hsp90 prepares the mitochondrial outer membrane translocon receptor Tom71 for preprotein loading.* J Biol Chem, 2009. **284**(35): p. 23852-9.
12. Wu, Y. and B. Sha, *Crystal structure of yeast mitochondrial outer membrane translocon member Tom70p.* Nat Struct Mol Biol, 2006. **13**(7): p. 589-93.
13. Backes, S., et al., *Tom70 enhances mitochondrial preprotein import efficiency by binding to internal targeting sequences.* J Cell Biol, 2018. **217**(4): p. 1369-1382.
14. Jores, T., et al., *Characterization of the targeting signal in mitochondrial beta-barrel proteins.* Nat Commun, 2016. **7**: p. 12036.
15. Brix, J., et al., *Distribution of binding sequences for the mitochondrial import receptors Tom20, Tom22, and Tom70 in a presequence-carrying preprotein and a non-cleavable preprotein.* J Biol Chem, 1999. **274**(23): p. 16522-30.
16. Aravindan, N., et al., *Mpf1 affects the dual distribution of tail-anchored proteins between mitochondria and peroxisomes.* EMBO Rep, 2025. **26**(10): p. 2622-2653.
17. Kondo-Okamoto, N., J.M. Shaw, and K. Okamoto, *Tetratricopeptide repeat proteins Tom70 and Tom71 mediate yeast mitochondrial morphogenesis.* EMBO Rep, 2008. **9**(1): p. 63-9.
18. Schlossmann, J., et al., *Tom71, a novel homologue of the mitochondrial preprotein receptor Tom70.* J Biol Chem, 1996. **271**(30): p. 17890-5.

19. Nowicka, U., et al., *Cytosolic aggregation of mitochondrial proteins disrupts cellular homeostasis by stimulating the aggregation of other proteins.* Elife, 2021. **10**.
20. Kaushik, P., J.M. Herrmann, and K.G. Hansen, *MitoStores: stress-induced aggregation of mitochondrial proteins.* Biol Chem, 2025. **406**(5-7): p. 237-249.
21. Boos, F., J. Labbadia, and J.M. Herrmann, *How the Mitoprotein-Induced Stress Response Safeguards the Cytosol: A Unified View.* Trends Cell Biol, 2020. **30**(3): p. 241-254.
22. Topf, U., B. Uszczynska-Ratajczak, and A. Chacinska, *Mitochondrial stress-dependent regulation of cellular protein synthesis.* J Cell Sci, 2019. **132**(8).
23. Wrobel, L., et al., *Mistargeted mitochondrial proteins activate a proteostatic response in the cytosol.* Nature, 2015. **524**(7566): p. 485-8.
24. Wang, X. and X.J. Chen, *A cytosolic network suppressing mitochondria-mediated proteostatic stress and cell death.* Nature, 2015. **524**(7566): p. 481-4.
25. Gautschi, M., et al., *RAC, a stable ribosome-associated complex in yeast formed by the DnaK-DnaJ homologs Ssz1p and zuotin.* Proc Natl Acad Sci U S A, 2001. **98**(7): p. 3762-7.
26. Yan, W., et al., *Zuotin, a ribosome-associated DnaJ molecular chaperone.* EMBO J, 1998. **17**(16): p. 4809-17.
27. Huang, P., et al., *The Hsp70 Ssz1 modulates the function of the ribosome-associated J-protein Zuo1.* Nat Struct Mol Biol, 2005. **12**(6): p. 497-504.
28. Lee, K., et al., *Pathway of Hsp70 interactions at the ribosome.* Nat Commun, 2021. **12**(1): p. 5666.
29. Black, A., et al., *The ribosome-associated chaperone Zuo1 controls translation upon TORC1 inhibition.* EMBO J, 2023. **42**(24): p. e113240.
30. Kisonaite, M., et al., *Structural inventory of cotranslational protein folding by the eukaryotic RAC complex.* Nat Struct Mol Biol, 2023. **30**(5): p. 670-677.
31. De Magis, A., et al., *Zuo1 supports G4 structure formation and directs repair toward nucleotide excision repair.* Nat Commun, 2020. **11**(1): p. 3907.
32. Yamamoto, A., Y. Mizukami, and H. Sakurai, *Identification of a novel class of target genes and a novel type of binding sequence of heat shock transcription factor in Saccharomyces cerevisiae.* J Biol Chem, 2005. **280**(12): p. 11911-9.
33. Kramer, L., et al., *MitoStores: chaperone-controlled protein granules store mitochondrial precursors in the cytosol.* EMBO J, 2023. **42**(7): p. e112309.
34. Boos, F., et al., *Mitochondrial protein-induced stress triggers a global adaptive transcriptional programme.* Nat Cell Biol, 2019. **21**(4): p. 442-451.
35. Young, J.C., N.J. Hoogenraad, and F.U. Hartl, *Molecular chaperones Hsp90 and Hsp70 deliver preproteins to the mitochondrial import receptor Tom70.* Cell, 2003. **112**(1): p. 41-50.
36. Schlossmann, J., et al., *Specific recognition of mitochondrial preproteins by the cytosolic domain of the import receptor MOM72.* J Biol Chem, 1994. **269**(16): p. 11893-901.
37. Brix, J., K. Dietmeier, and N. Pfanner, *Differential recognition of preproteins by the purified cytosolic domains of the mitochondrial import receptors Tom20, Tom22, and Tom70.* J Biol Chem, 1997. **272**(33): p. 20730-5.
38. Costa-Mattioli, M. and P. Walter, *The integrated stress response: From mechanism to disease.* Science, 2020. **368**(6489).

39. Pakos-Zebrucka, K., et al., *The integrated stress response.* EMBO Rep, 2016. **17**(10): p. 1374-1395.
40. Guo, X., et al., *Mitochondrial stress is relayed to the cytosol by an OMA1-DELE1-HRI pathway.* Nature, 2020. **579**(7799): p. 427-432.
41. Romanelli, S. and J.F. Trempe, *Stressful situations: Molecular insights on mitochondrial quality control pathways.* J Biol Chem, 2025. **301**(8): p. 110483.
42. Rodrigues, J.I., et al., *Yeast chaperones and ubiquitin ligases contribute to proteostasis during arsenite stress by preventing or clearing protein aggregates.* FEBS Lett, 2023. **597**(13): p. 1733-1747.
43. Albanese, V., S. Reissmann, and J. Frydman, *A ribosome-anchored chaperone network that facilitates eukaryotic ribosome biogenesis.* J Cell Biol, 2010. **189**(1): p. 69-81.
44. Cashikar, A.G., M. Duennwald, and S.L. Lindquist, *A chaperone pathway in protein disaggregation. Hsp26 alters the nature of protein aggregates to facilitate reactivation by Hsp104.* J Biol Chem, 2005. **280**(25): p. 23869-75.
45. Welker, S., et al., *Hsp12 is an intrinsically unstructured stress protein that folds upon membrane association and modulates membrane function.* Mol Cell, 2010. **39**(4): p. 507-20.
46. Borchert, N., et al., *Proteogenomics of Pristionchus pacificus reveals distinct proteome structure of nematode models.* Genome Res, 2010. **20**(6): p. 837-46.
47. Rappsilber, J., M. Mann, and Y. Ishihama, *Protocol for micro-purification, enrichment, pre-fractionation and storage of peptides for proteomics using StageTips.* Nat Protoc, 2007. **2**(8): p. 1896-906.
48. Baker, C.P., et al., *Optimizing Spectronaut Search Parameters to Improve Data Quality with Minimal Proteome Coverage Reductions in DIA Analyses of Heterogeneous Samples.* J Proteome Res, 2024. **23**(6): p. 1926-1936.
49. Huber, W., et al., *Variance stabilization applied to microarray data calibration and to the quantification of differential expression.* Bioinformatics, 2002. **18 Suppl 1**: p. S96-104.
50. Ritchie, M.E., et al., *limma powers differential expression analyses for RNA-sequencing and microarray studies.* Nucleic Acids Res, 2015. **43**(7): p. e47.
51. Eden, E., et al., *GOrilla: a tool for discovery and visualization of enriched GO terms in ranked gene lists.* BMC Bioinformatics, 2009. **10**: p. 48.

512 # Figure legends

513

514 **Figure 1.**

515 **Cells deleted for *ZUO1* display retarded growth at 30°C.** (**A** and **B**) The growth of the
516 indicated strains at 30°C in rich liquid medium containing either glucose (A, YPD) or galactose
517 (B, YPGal) was monitored using OD_{600} measurements for 24 or 40 hours, respectively. At the
518 beginning of the measurements (time 0), the strains were diluted to an OD_{600} of 0.1. (**C**) The
519 growth of the indicated strains was monitored at 30°C by drop dilution assay on solid rich
520 medium containing glucose (YPD), galactose (YPGal), or glycerol (YPG). Plates were
521 incubated for one or two days before pictures were taken.

522

523 **Figure 2.**

524 **The absence of Zuo1 at elevated temperature restores the compromised growth of**
525 ***tom70Δ/tom71Δ* cells.** (**A** and **B**) The growth of the indicated strains at 37°C was monitored as
526 described in Fig.1A, B. (**C**) The growth of the indicated strains was monitored at 37°C by drop
527 dilution assay as described in Fig. 1C.

528

529 **Figure 3.**

530 **The absence of Zuo1 does not restore the depletion of mitochondrial proteins in**
531 ***tom70Δ/tom71Δ* cells.** (**A**) Scheme of the mass spectrometry measurement of cellular proteins.
532 (**B**) Principal Component Analysis. (**C**) Venn diagrams showing the number of proteins that
533 were identified in the different replicates. (**D**) Volcano plots comparing the proteomes of the
534 indicated strains. Mitochondrial proteins are shown in blue. (**E**) Violin plots to compare the
535 abundance of non-mitochondrial and mitochondrial (in blue) proteins in the different strains. A
536 two-sided wilcoxon rank sum test with continuity correction was used to calculate p-values for
537 indicated comparisons. (**F**) Enrichment of gene ontology terms was performed for the most
538 extremely depleted proteins (log_2 fold change > -0.8 in the limma analysis) using the GOrilla
539 website (http://cbl-gorilla.cs.technion.ac.il); see Suppl. Table 3 for details. WT, wildtype, ΔΔ,
540 *tom70Δ/tom71Δ*, ΔΔΔ, *tom70Δ/tom71Δ/zuo1Δ*.

541

542

543 **Figure 4.**

544 **Deletion of *TOM70/71* and *ZUO1* leaves a characteristic footprint on the proteostasis**
545 **network.** (**A**) Scheme of the heat response program. **(B)** Violin plots comparing the abundance
546 of proteins that are heat shock regulated (in orange, see [32] and Suppl. Table 2) to non-heat
547 shock regulated proteins in the different strains. **(C** and **D)** Volcano plots demonstrating that
548 deletion of *TOM70/71* leads to a marked upregulation of heat shock regulated proteins but not
549 additional deletion of *ZUO1*. WT, wildtype, ΔΔ, *tom70Δ/tom71Δ*, ΔΔΔ,
550 *tom70Δ/tom71Δ/zuo1Δ*.

551

552 **Figure 5.**

553 **The additional deletion of *ZUO1* differentially affects the levels of cytosolic chaperones.**
554 **(A)** Proteins were extracted from the indicated strains and analyzed by SDS-PAGE and
555 immunodecorated with the indicated antibodies. (**B**) The bands corresponding to the indicated
556 proteins from three independent experiments as the one shown in (A) were quantified and
557 normalized to the intensities of the Ponceau S staining. The value of the WT cells was set as
558 100%. The bar diagram shows the average ± SD of three independent experiments.

559

560 **Figure 6.**

561 **Removal of Zuo1 affects to a different extent the levels of mitochondrial outer membrane**
562 **proteins. (A)** Proteins were extracted from the indicated strains and analyzed by SDS-PAGE
563 and immunodecorated with the indicated antibodies. (**B**) The bands corresponding to the
564 indicated proteins from three independent experiments as the one shown in (A) were quantified
565 and normalized to the intensities of the Ponceau S staining. The value of the WT cells was set
566 as 100%. The bar diagram shows the average ± SD of three independent experiments.

567

568 **Figure 7.**

569 **Deletion of *TOM70/71* leads to the formation of cytosolic aggregates and slows down**
570 **protein synthesis.** (**A**) Strains expressing Hsp104-GFP were analyzed by fluorescence
571 microscopy. Hsp104-bound aggregates are indicated with yellow arrows. Scale bars, 5 µm. (**B**)
572 Quantification of cells containing aggregates. Cell populations were categorized into cells with
573 no aggregates (dark blue), with 1-4 aggregates (medium blue), or with ≥5 aggregates (light

574 blue). The portion of cells in each category is shown as percentage of all cells counted with n
575 = 137 for WT, n = 182 for *zuo1Δ*, n = 145 for *tom70Δ/tom71Δ,* and n = 297 for the triple mutant.
576 (**C**) *In vivo* labeling of newly synthesized proteins at 30°C in media containing either glucose
577 or galactose for either 5 or 15 minutes. Proteins were analyzed by SDS-PAGE and the
578 radiolabeled translation products of the different strains were detected by autoradiography.
579 Immunostaining against Rpl6b is shown as a loading control. (**D**) The signal of all detected
580 proteins for a certain lane as in (C) was quantified and normalized to the loading control Rpl6b.
581 The indicated data points at 5 and 15 min represent the relevant intensity of the radiolabeled
582 translation products of three biological replicates. The intensity of the translation products in
583 WT cells after 15 min was set to 1. Error bars represent ±S.D. (**E**) Cells were grown at the
584 indicated temperature on glucose as a carbon source. Radiolabeled translation products after a
585 labelling period of either 2 or 10 min were analyzed by dot blot and autoradiography. (**F**) Model
586 showing that the deletion of *ZUO1* leads to the remodeling of the cytosolic stress response.

A

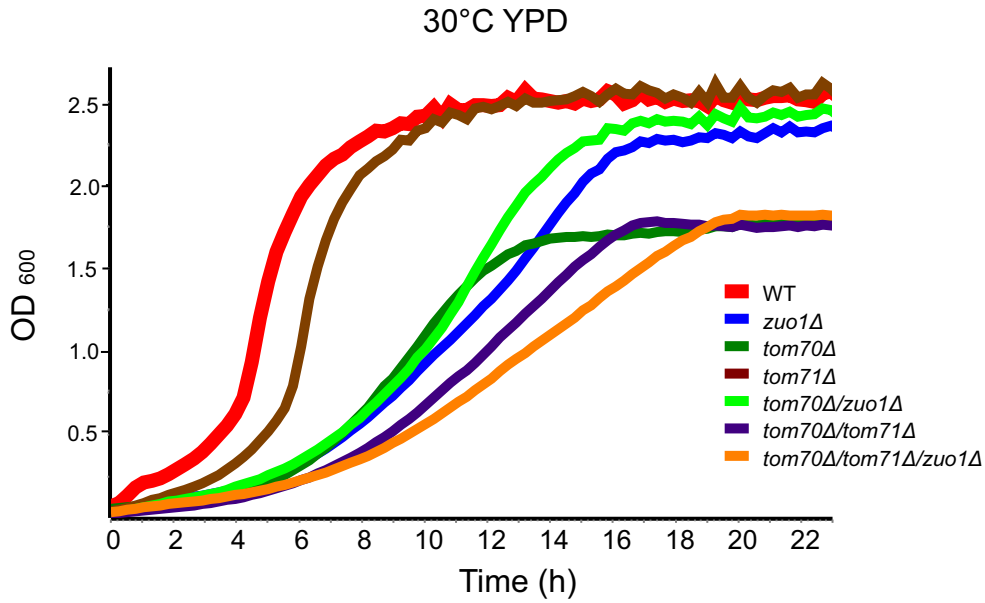

B

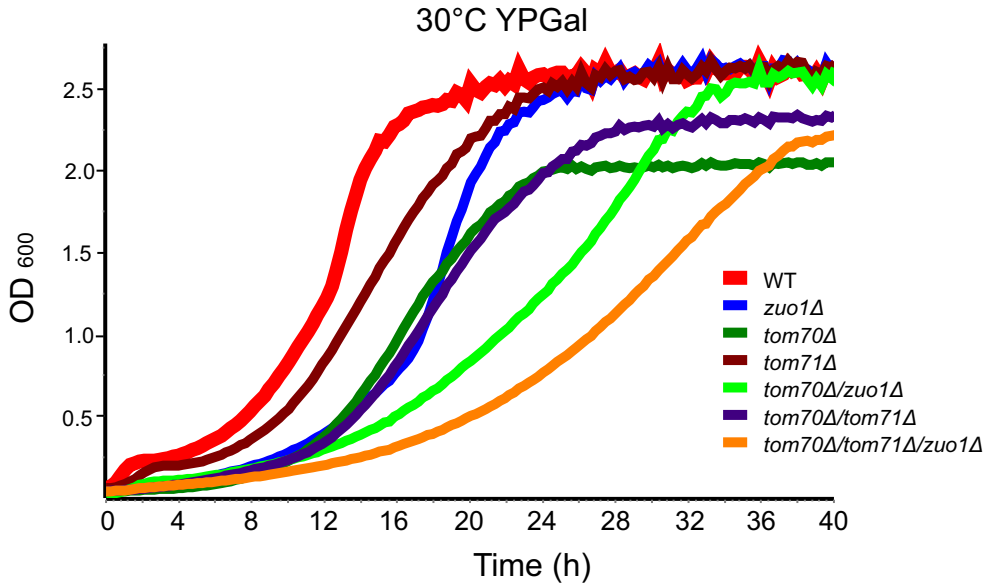

C

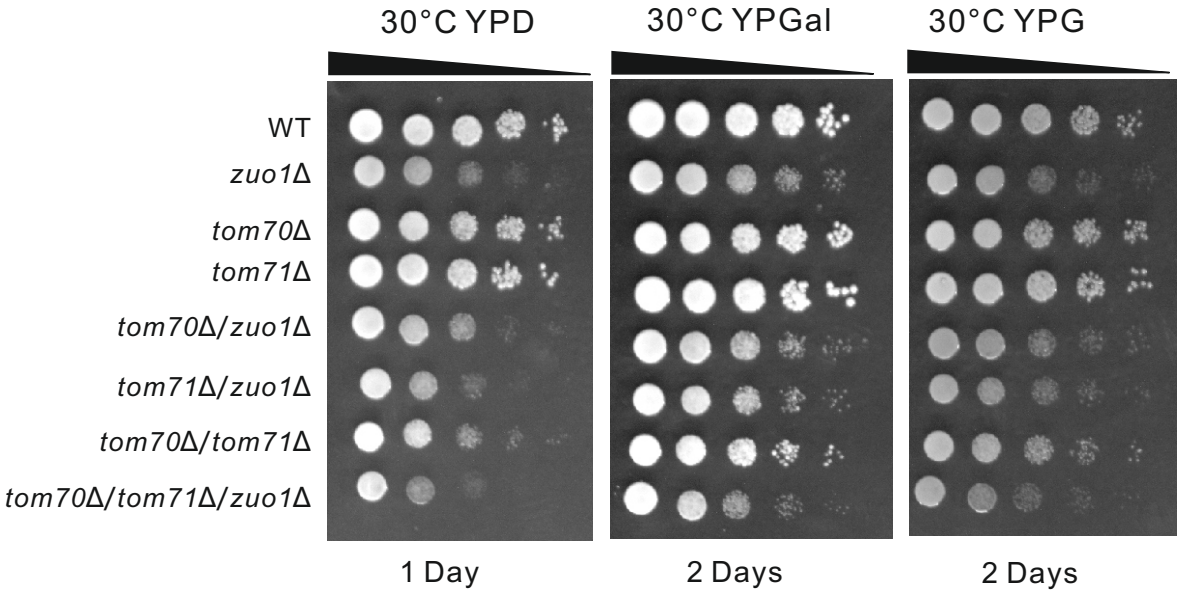

Qian et al., Fig. 1

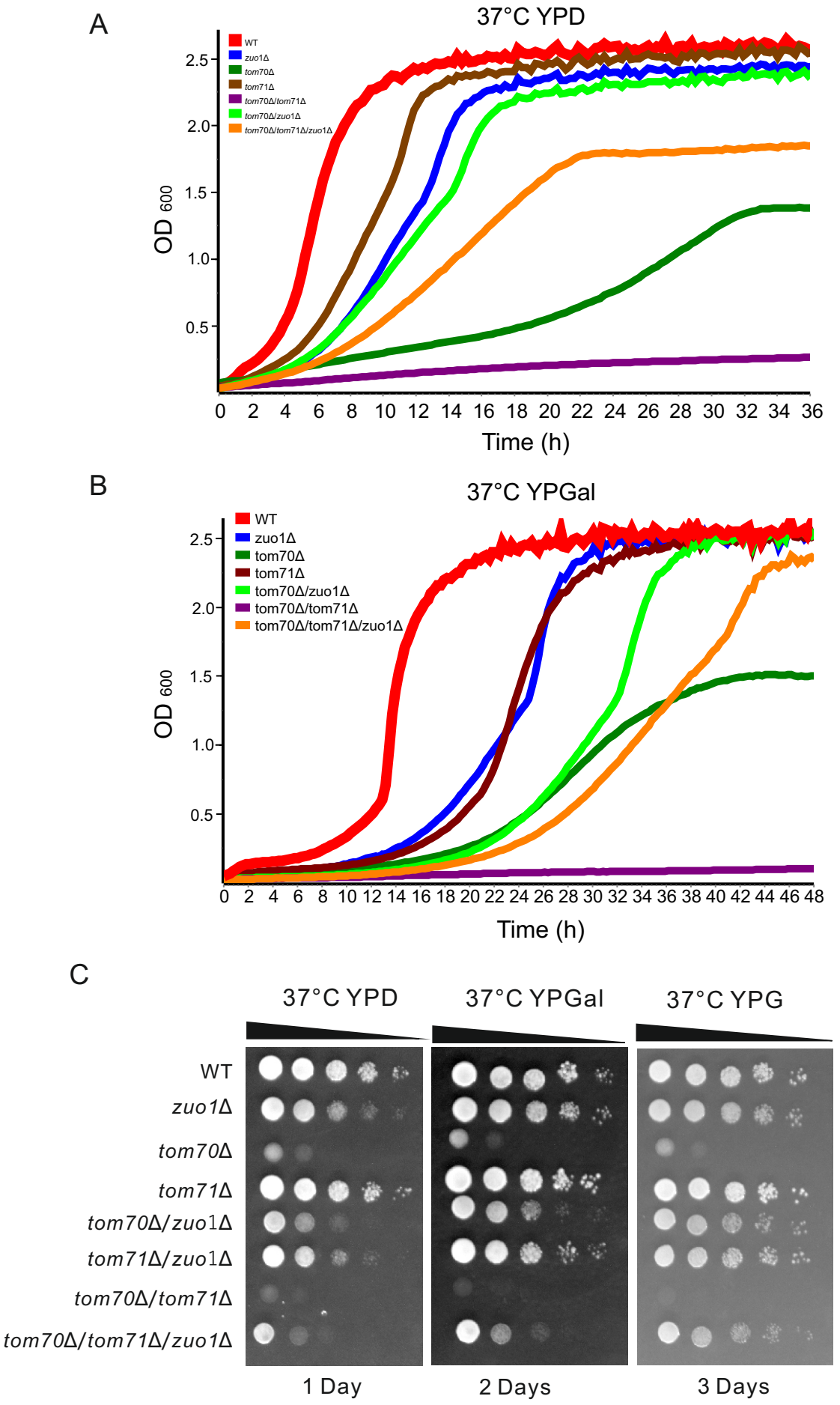

Qian et al., Fig. 2

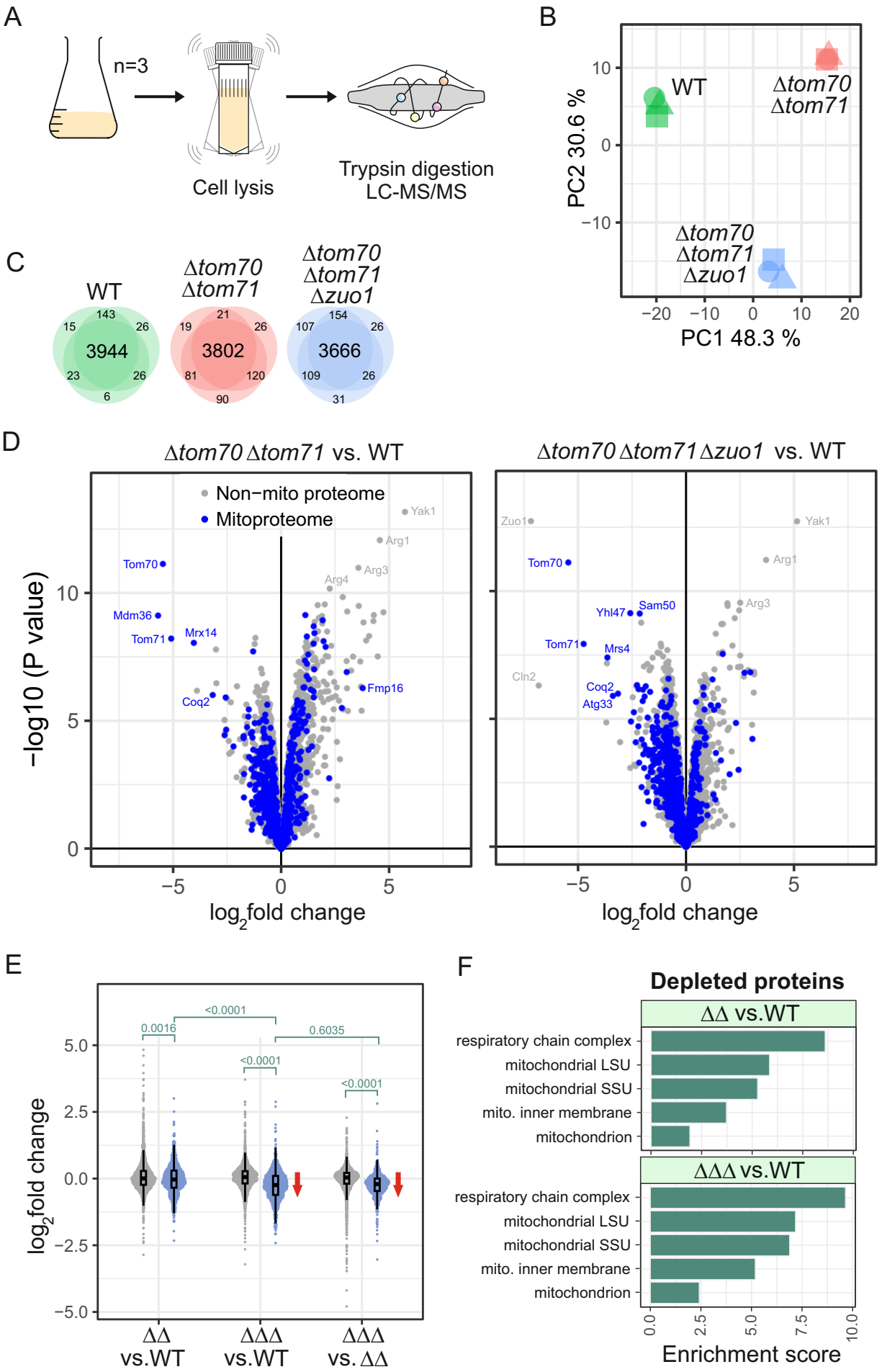

Qian et al., Fig. 3

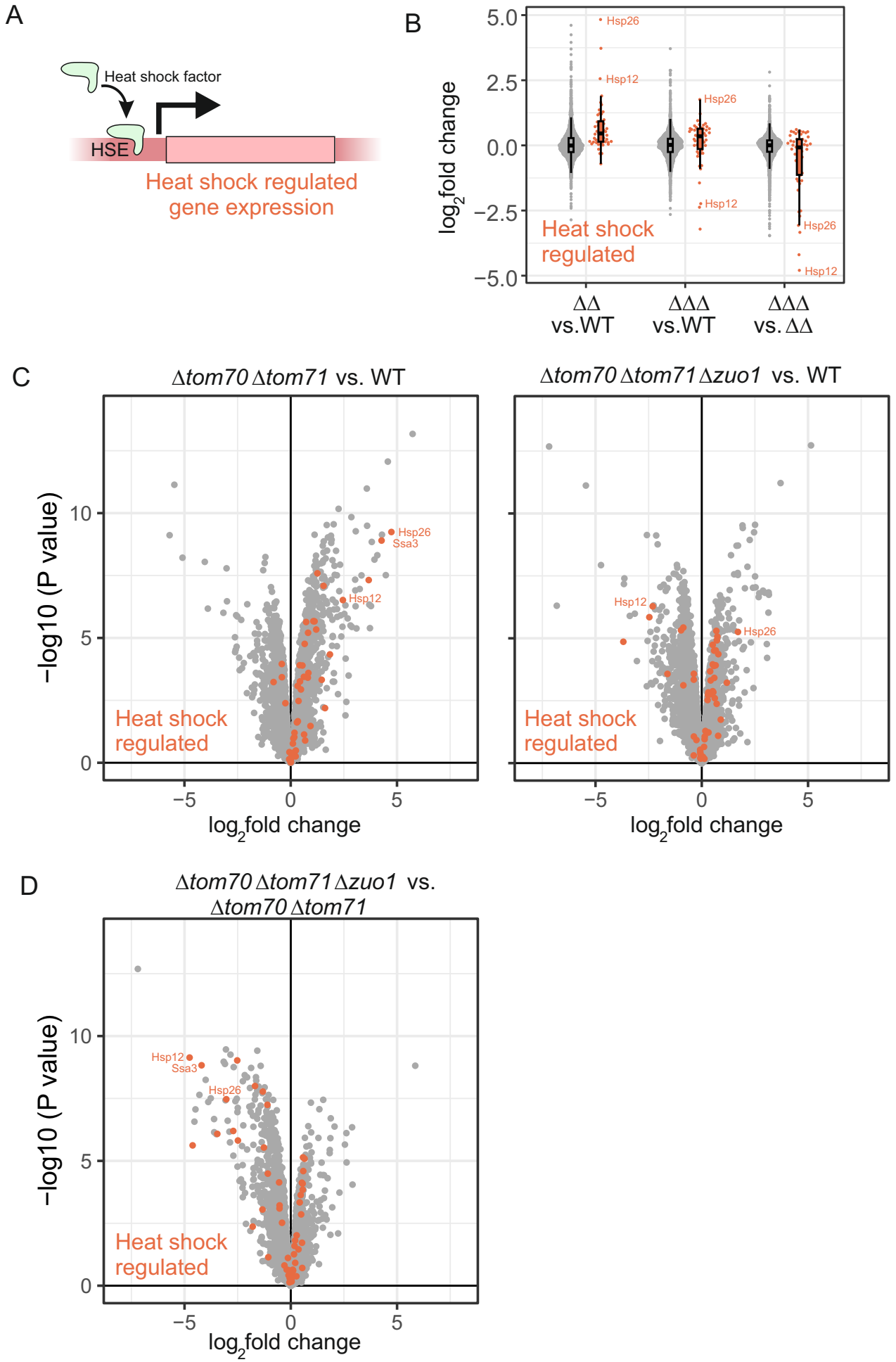

Qian et al., Fig. 4

A

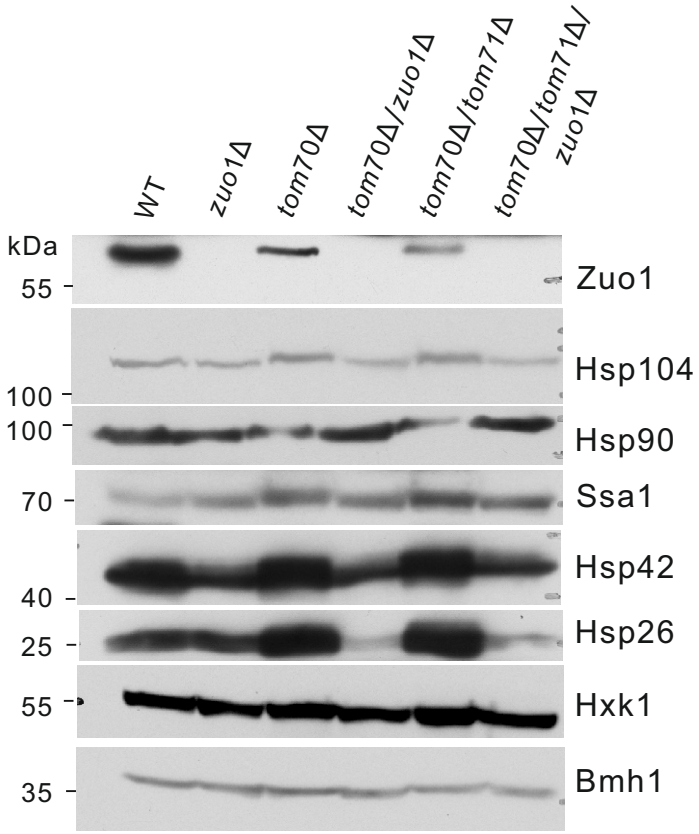

B

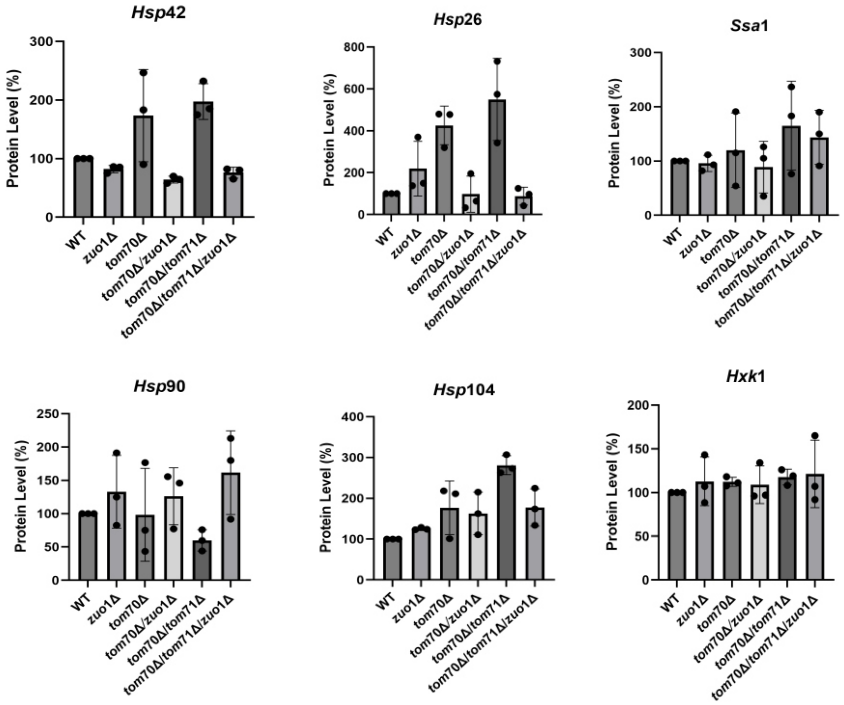

Qian et al., Fig. 5

A

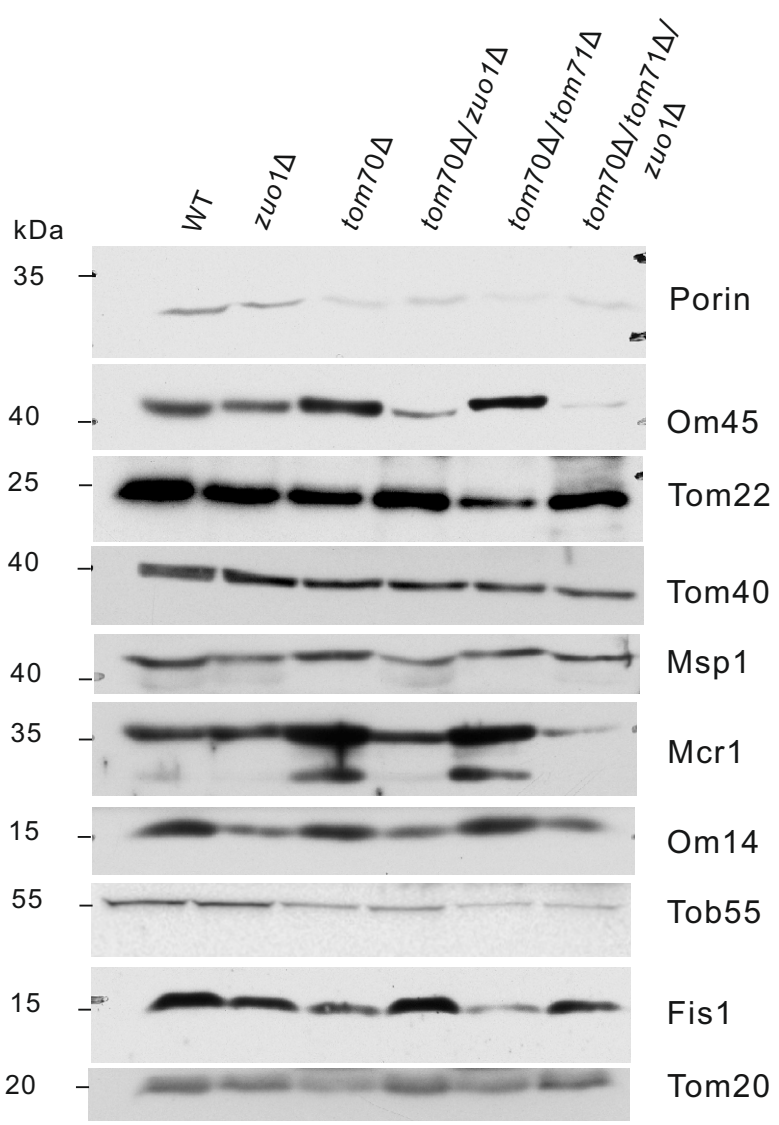

B

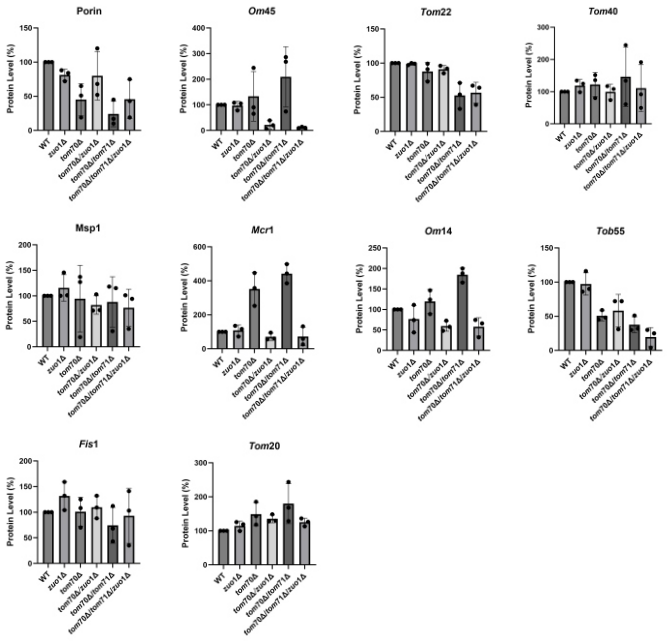

Qian et al., Fig. 6

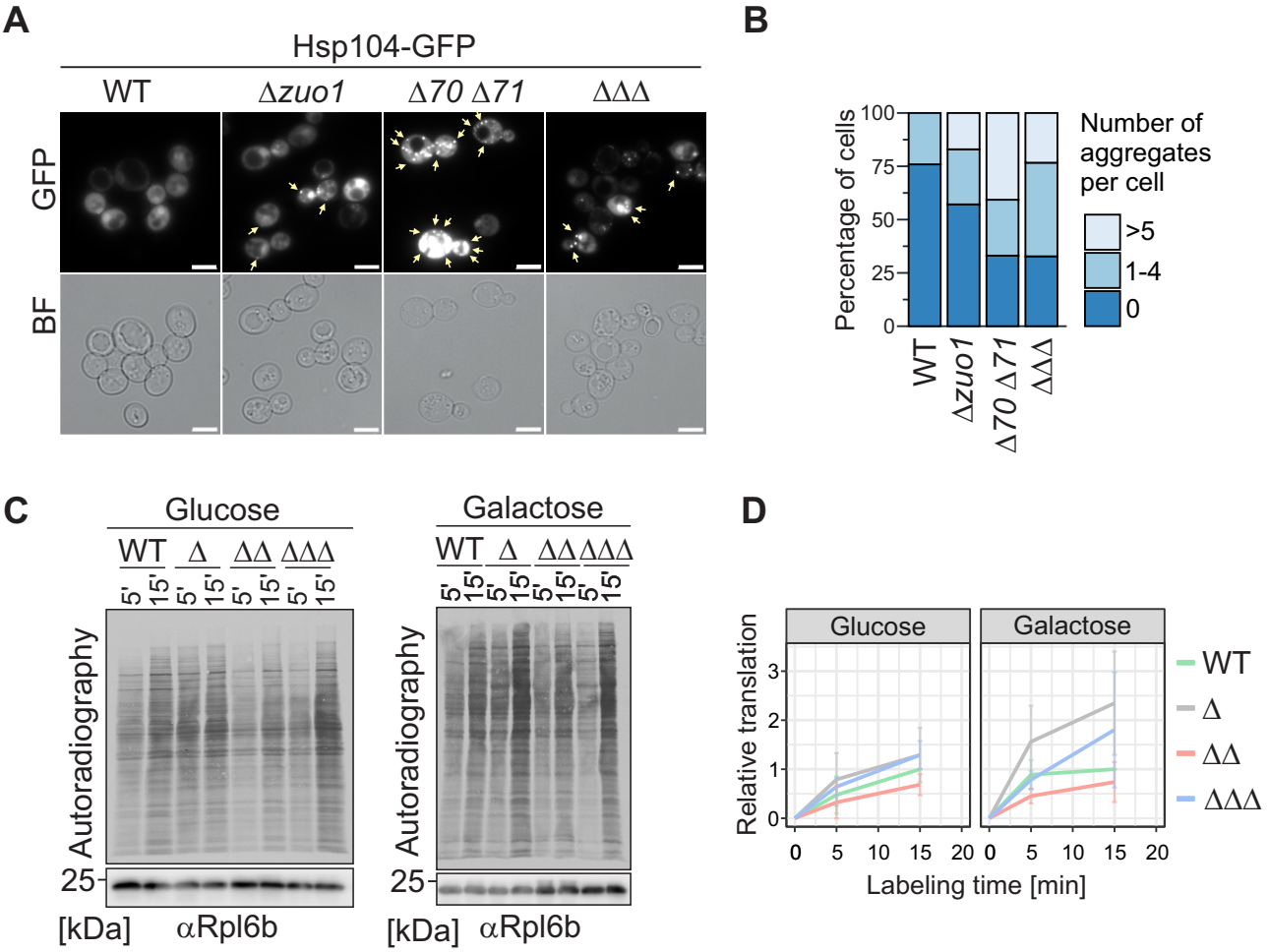

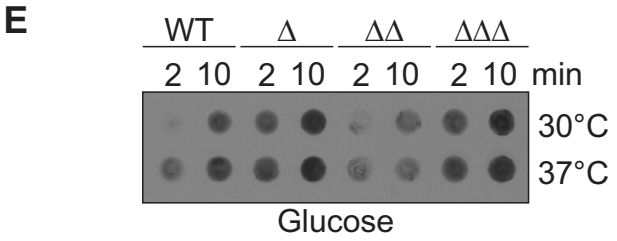

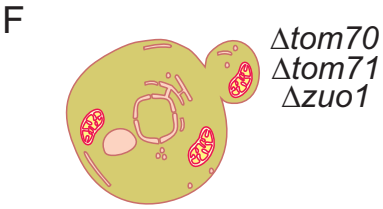

Model:
ZUO1 deletion leads to remodeling of the cytosolic stress response

Qian et al., Fig. 7